Table S1. Vertical levels for the WRF simulation.

Level	η	Approximate height of the midpoint of the layer AGL (m)	Level	η	Approximate height of the midpoint of the layer AGL (m)
0	1.0000	0	16	0.7100	2,341
1	0.9975	10	17	0.6100	3,130
2	0.9950	30	18	0.5100	4,272
3	0.9925	50	19	0.4100	5,563
4	0.9900	70	20	0.3600	6,635
5	0.9875	90	21	0.2950	7,568
6	0.9850	110	22	0.2550	8,490
7	0.9800	140	23	0.2200	9,215
8	0.9700	200	24	0.1900	9,894
9	0.9550	301	25	0.1650	10,511
10	0.9350	444	26	0.1450	11,052
11	0.9100	631	27	0.1250	11,566
12	0.8800	864	28	0.1050	12,118
13	0.8450	1,145	29	0.0800	12,800
14	0.8100	1,458	30	0.0500	13,740
15	0.7600	1,854	31	0.0000	15,467

5   **Table S2. Summary of WRF parameterizations.**

Parameter	Option
Shortwave Radiation	MM5 Shortwave radiation scheme (Dudhia, 1989)
Longwave Radiation	Rapid Radiative Transfer Model (RRTM) (Mlawer et al., 1997)
Surface Model	Noah LSM (Alapaty et al., 2008)
Microphysics	WSM6 (Hong & Lim, 2006)
PBL	Yonsei University (YSU) (Hong, Noh & Dudhia, 2006)
SST	OISST (Reynolds et al., 2007)

Table S3. CAMx and WRF correspondence levels.

CAMx level	WRF level	Approximate height of the layer interface AGL (m)
1	1	20
2	2	40
3	3	60
4	4	80
5	7	160
6	8	220
7	9	350
8	10	530
9	11	730
10	12	1,000
11	14	1,600
12	16	2,500
13	17	3,600
14	18	4,800

Table S4. Statistical metrics for the selected O₃ measurement stations with its codification and location coordinates in Northern Atlantic Iberia (NAI). The station of Valderejo in the Valderejo Natural Park (VNP) is highlighted in gray.

Station Code	Latitude (degrees)	Longitude (degrees)	MB ($\mu g \cdot m^{-3}$)	ME ($\mu g \cdot m^{-3}$)	NMB	IOA	r
ES0005R	42.72	-8.92	3	15	4%	0.82	0.72
ES0008R	43.44	-4.85	7	12	10%	0.76	0.67
ES0016R	42.63	-7.70	26	27	46%	0.57	0.44
ES0094A	43.41	-7.99	5	16	6%	0.77	0.61
ES0201A	43.45	-7.85	13	26	25%	0.67	0.53
ES0339A	43.69	-7.51	32	32	66%	0.43	0.57
ES0354A	42.88	-6.44	41	41	80%	0.45	0.49
ES0360A	42.78	-6.60	16	21	21%	0.61	0.48
ES0365A	42.70	-4.83	9	28	12%	0.52	0.47
ES0373A	42.63	-6.52	14	22	20%	0.63	0.44
ES0377A	42.61	-6.64	12	23	17%	0.70	0.59
ES0587A	43.32	-3.11	4	21	6%	0.80	0.64
ES0761A	42.72	-5.64	27	28	44%	0.61	0.61
ES0824A	43.31	-5.71	24	33	47%	0.61	0.45
ES0825A	43.31	-5.69	27	34	55%	0.58	0.42
ES0879A	43.55	-5.90	-3	20	-5%	0.70	0.50
ES0880A	43.55	-5.92	-4	24	-8%	0.59	0.35
ES0901A	43.24	-8.32	20	25	36%	0.77	0.76
ES0961A	42.43	-8.68	6	29	7%	0.64	0.56
ES1038A	43.35	-4.06	33	36	67%	0.60	0.52
ES1137A	42.22	-8.74	26	34	44%	0.62	0.49
ES1138A	43.37	-8.42	26	31	62%	0.53	0.42
ES1175A	42.72	-7.45	35	38	69%	0.49	0.20
ES1268A	43.36	-5.87	-12	28	-19%	0.71	0.54
ES1269A	43.37	-5.83	3	26	7%	0.72	0.55
ES1270A	43.54	-5.66	-3	25	-7%	0.56	0.33
ES1271A	43.54	-5.70	-21	27	-30%	0.56	0.43
ES1285A	43.53	-7.74	14	21	21%	0.52	0.30
ES1287A	42.80	-4.84	18	23	27%	0.59	0.57
ES1297A	42.80	-5.62	6	19	7%	0.67	0.55
ES1346A	42.69	-2.94	12	24	16%	0.70	0.64
ES1349A	43.14	-2.96	45	46	92%	0.60	0.61
ES1353A	43.29	-5.68	17	29	30%	0.64	0.45
ES1358A	43.54	-5.65	-1	17	-2%	0.69	0.47
ES1359A	43.31	-7.69	30	30	57%	0.60	0.51
ES1424A	43.56	-5.93	8	22	20%	0.58	0.41
ES1432A	43.18	-6.55	41	42	81%	0.53	0.59
ES1439A	42.20	-8.75	25	35	38%	0.62	0.50
ES1472A	42.81	-1.65	11	17	14%	0.78	0.73
ES1489A	**42.88**	**-3.23**	**4**	**20**	**4%**	**0.77**	**0.68**

Station Code	Latitude (degrees)	Longitude (degrees)	MB ($\mu g \cdot m^{-3}$)	ME ($\mu g \cdot m^{-3}$)	NMB	IOA	r
ES1490A	43.17	-2.64	45	45	103%	0.57	0.67
ES1491A	43.41	-2.70	10	16	13%	0.76	0.74
ES1501A	43.18	-2.27	38	41	66%	0.54	0.38
ES1529A	43.47	-3.79	13	15	20%	0.76	0.71
ES1530A	43.01	-4.14	24	26	35%	0.66	0.62
ES1531A	43.15	-4.25	21	24	29%	0.65	0.59
ES1544A	42.85	-2.39	16	28	21%	0.64	0.59
ES1557A	43.26	-8.56	28	31	48%	0.51	0.38
ES1576A	43.40	-3.84	37	37	84%	0.57	0.61
ES1577A	43.42	-3.84	27	28	50%	0.63	0.61
ES1578A	43.38	-3.22	20	23	35%	0.73	0.71
ES1579A	43.26	-4.06	50	50	120%	0.53	0.53
ES1591A	42.56	-6.73	26	36	42%	0.56	0.46
ES1598A	43.21	-3.13	24	33	34%	0.63	0.46
ES1599A	43.25	-2.16	0	14	0%	0.83	0.74
ES1651A	43.26	-5.78	19	30	37%	0.65	0.48
ES1696A	43.30	-1.98	24	27	40%	0.62	0.59
ES1697A	43.31	-2.01	24	28	41%	0.60	0.54
ES1713A	43.25	-2.90	37	37	89%	0.62	0.64
ES1740A	42.81	-1.64	29	30	53%	0.61	0.64
ES1747A	42.83	-1.65	10	15	14%	0.79	0.74
ES1749A	42.90	-2.17	27	33	40%	0.57	0.42
ES1790A	42.54	-6.58	25	31	40%	0.59	0.51
ES1867A	43.48	-8.24	31	31	56%	0.46	0.29
ES1868A	42.88	-8.56	14	23	21%	0.70	0.56
ES1901A	42.89	-8.53	18	28	28%	0.63	0.47
ES1905A	43.00	-7.55	40	40	102%	0.44	0.35
ES1907A	43.30	-8.51	25	27	61%	0.71	0.70
ES1957A	43.38	-8.41	25	25	46%	0.60	0.63
ES1960A	43.49	-8.25	18	21	27%	0.54	0.32
ES1974A	43.52	-5.67	-6	20	-11%	0.76	0.61
ES1987A	42.95	-3.48	14	21	18%	0.71	0.57
ES1988A	42.58	-5.57	11	21	15%	0.76	0.75
ES1989A	43.04	-5.09	34	34	63%	0.44	0.08
ES2014A	42.06	-7.41	16	18	21%	0.61	0.52
ES2015A	42.18	-8.52	43	47	93%	0.57	0.55
ES2049A	43.12	-8.35	11	23	15%	0.69	0.51
ES2051A	43.40	-5.80	6	26	13%	0.70	0.55
ES2054A	43.57	-5.96	20	25	50%	0.70	0.62
ES2058A	43.26	-2.97	35	36	72%	0.63	0.65
ES2075A	43.35	-5.97	25	28	55%	0.70	0.62
ES2083A	43.07	-6.19	24	28	34%	0.58	0.53
ES2085A	42.06	-7.73	29	33	51%	0.57	0.38

15 **Table S5. Statistical metrics for the selected O$_3$ measurement stations with its codification and location coordinates in Western Atlantic Iberia (WAI). The station of Douro Norte (DN) in Alvão Natural Park is highlighted in gray.**

Station Code	Latitude (degrees)	Longitude (degrees)	MB (µg·m^{-3})	ME (µg·m^{-3})	NMB	IOA	r
PT01034	41.22	-8.63	-1	21	-1%	0.88	0.85
PT01044	41.27	-8.38	68	68	293%	0.40	0.48
PT01047	41.80	-8.70	40	41	78%	0.36	0.17
PT01048	**41.37**	**-7.79**	**1**	**11**	**1%**	**0.87**	**0.79**
PT01050	41.15	-8.66	8	22	14%	0.83	0.72
PT02004	40.76	-8.57	21	32	35%	0.76	0.82
PT02016	40.21	-8.41	7	21	9%	0.82	0.83
PT02018	40.59	-8.67	18	30	26%	0.75	0.82
PT02020	40.23	-7.30	23	26	36%	0.53	0.32
PT02022	40.18	-8.68	-11	21	-11%	0.75	0.78
PT03063	38.62	-9.08	14	21	22%	0.82	0.80
PT03070	38.73	-9.11	1	16	1%	0.85	0.78
PT03071	38.77	-9.11	11	20	16%	0.76	0.68
PT03072	38.75	-9.15	9	19	14%	0.80	0.73
PT03082	38.74	-9.21	9	24	13%	0.78	0.71
PT03083	38.66	-9.16	11	22	15%	0.81	0.80
PT03084	38.75	-9.23	-11	16	-12%	0.81	0.77
PT03085	38.83	-9.17	-7	15	-9%	0.83	0.76
PT03087	38.71	-9.21	3	19	4%	0.81	0.74
PT03089	38.78	-9.35	-14	17	-14%	0.77	0.68
PT03091	38.70	-9.32	-5	15	-5%	0.83	0.72
PT03093	38.53	-8.89	-13	19	-15%	0.80	0.77
PT03095	38.66	-9.07	-4	19	-5%	0.83	0.82
PT03096	39.35	-8.47	-27	27	-25%	0.66	0.73
PT03099	38.64	-8.69	-3	15	-4%	0.81	0.77
PT03101	38.90	-9.04	-1	18	-1%	0.75	0.66
PT03102	39.28	-9.25	-14	19	-15%	0.73	0.75
PT04001	37.95	-8.84	-75	75	-70%	0.40	0.38
PT04002	38.08	-8.80	-69	76	-46%	0.53	0.70
PT04006	38.62	-7.40	23	27	39%	0.52	0.42
PT05007	37.01	-7.93	-7	14	-7%	0.80	0.74
PT05008	37.09	-8.25	-4	10	-5%	0.87	0.79
PT05012	37.31	-7.68	-16	17	-16%	0.73	0.76
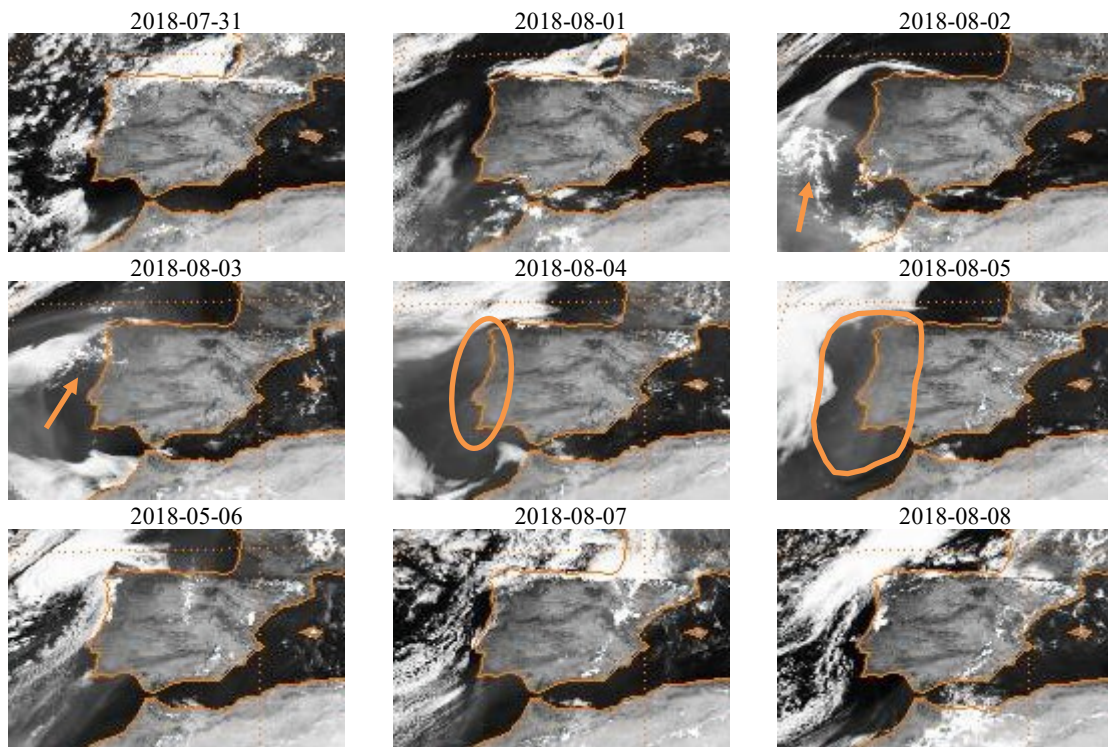
Figure S1. Satellite imagery from the Meteosat visible channel by NOAA's Global ISCCP B1 Browse System at daily 12 UTC from July 31 to August 8 (Knapp, 2008). Orange marks indicate the possible location of the Saharan dust transported to the Iberian Peninsula.

20
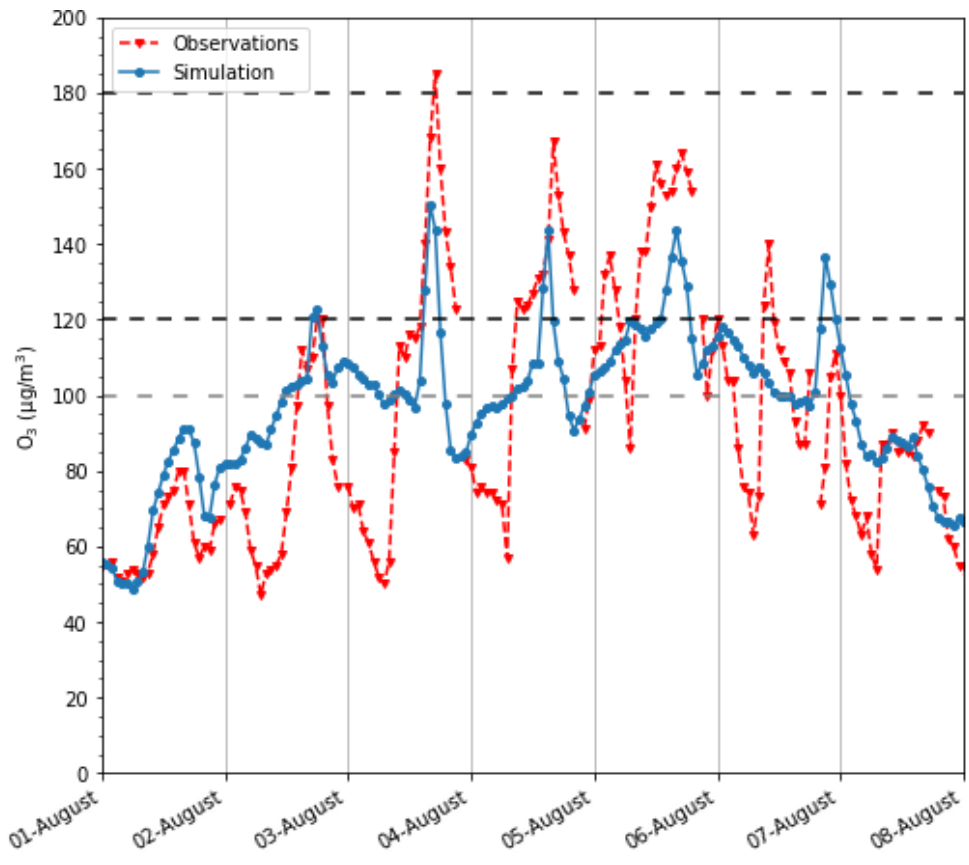
Figure S2. Comparison of the observed (red) and simulated (blue) hourly O₃ time series for the Valderejo Natural Park (VNP) station.

25
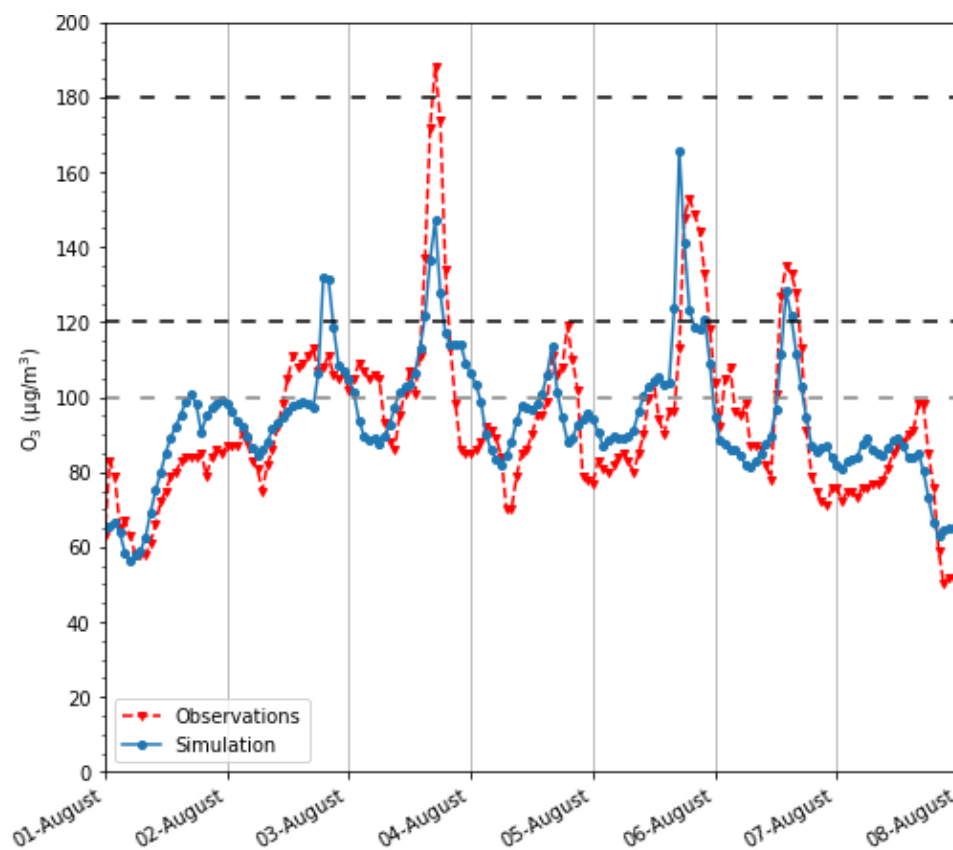
Figure S3. Comparison of the observed (red) and simulated (blue) hourly O₃ time series for the Douro Norte (DN) station.

30

References

Alapaty, K., Niyogi, D., Chen, F., Pyle, P., Chandrasekar, A., and Seaman, N.: Development of the Flux-Adjusting Surface Data Assimilation System for Mesoscale Models, Journal of Applied Meteorology and Climatology, 47(9), 2331-2350, https://doi.org/10.1175/2008JAMC1831.1, 2008.

35   Dudhia, J.: Numerical Study of Convection Observed during the Winter Monsoon Experiment Using a Mesoscale Two-Dimensional Model, Journal of the Atmospheric Sciences, 46(20), 3077-3107, https://doi.org/10.1175/1520-0469(1989)046<3077:NSOCOD>2.0.CO;2, 1989.

Hong, S. and Lim, J.: The WRF Single-Moment 6-Class Microphysics Scheme (WSM6), Journal of the Korean Meteorological Society, 42, 129-151, 2006.

40   Hong, S.-Y., Noh, Y., and Dudhia, J.: A New Vertical Diffusion Package with an Explicit Treatment of Entrainment Processes, Monthly Weather Review, 134, 2318-2341, http://dx.doi.org/10.1175/MWR3199.1, 2006.

Knapp, K. R.: Scientific data stewardship of International Satellite Cloud Climatology Project B1 global geostationary observations, Journal of Applied Remote Sensing, 2, 023548, http://doi:10.1117/1.3043461,
45   2008.

Mlawer, E. J., Taubman, S. J., Brown, P. D., Iacono, M. J., and Clough, S. A.: Radiative transfer for inhomogeneous atmospheres: RRTM, a validated correlated-k model for the longwave, Journal of Geophysical Research: Atmospheres, 102(D14), 16663-16682, https://doi.org/10.1029/97JD00237, 1997.

Reynolds, R. W., Smith, T. M., Liu, C., Chelton, D. B., Casey, K. S., and Schlax., M. G.: Daily high-
50   resolution-blended analyses for sea surface temperature, Journal of Climate, 20, 5473–5496, http://doi:10.1175/JCLI-D-14-00293.1, 2007.